Hindawi
Advances in Civil Engineering
Volume 2022, Article ID 5910701, 14 pages
https://doi.org/10.1155/2022/5910701

Research Article

The Impact of Molar Proportion of Sodium Hydroxide and Water Amount on the Compressive Strength of Slag/Metakaolin (Waste Materials) Geopolymer Mortar

Fatimah N. Al-Husseinawi,[1,2] **William Atherton**,[3] **Zainab Al-Khafaji**,[4] **Monower Sadique**,[3] and **Zaher Mundher Yaseen**[5]

[1]*Liverpool John Moores University, Department of Civil Engineering, Liverpool L3 3AF, UK*
[2]*Al-Turath University College, Baghdad, Iraq*
[3]*Liverpool John Moores University, Department of Civil Engineering, Peter Jost Enterprise Centre, Byrom Street, Liverpool L3 3AF, UK*
[4]*Building and Construction Techniques Engineering Department, AL-Mustaqbal University College, Hillah 51001, Iraq*
[5]*Civil and Environmental Engineering Department, King Fahd University of Petroleum & Minerals, Dhahran 31261, Saudi Arabia*

Correspondence should be addressed to Zaher Mundher Yaseen; yaseen@alayen.edu.iq

Received 28 June 2022; Accepted 21 September 2022; Published 6 October 2022

Academic Editor: Md. Akter Hosen

This investigation aimed to improve great early geopolymer mortar strengths under various parameters with various binder proportions to reduce the use of cement since the OPC production process leads to high emissions of CO_2. Hence, to solve this problem, alternative materials were used. In this research, metakaolin (MK) and ground-granulated blast-furnace slag (GGBFS) waste materials were utilized and mixed together with the sodium hydroxide and alkaline activator sodium silicate (NaOH and Na_2SiO_3). The performance of the various mixtures was assessed via compressive strength testing based on British standards. The compressive strength was found to be highly affected by molar proportion and water amount. The optimum strength was 77.8 MPa for a mix design of 95% GGBFS +5% MK and a 2.5 mass proportion between Na_2SiO_3 and NaOH (12 Molar), together with a 0.2 water/binder proportion.

1. Introduction

Owing to its excellent strength and durability, concrete seems to be the most extensively used material in building, with an expected current usage of 1 m^3 per person annually [1]. Concrete is produced mostly of cement, gravel, sand, and water, which has been used in the building of tunnels, skyscrapers, airports, residences, and other constructions. However, there are several challenges associated with the usage of ordinary Portland cement (OPC), including durability issues, including concrete disintegration when attacked by aggressive substances such as acids, sulphates, and chlorides [2–4]. In addition, the environmental concerns were raised by the release of around 5–7% of total global CO_2 emissions throughout the OPC manufacturing process and the usage of 5% of natural resources owing to the widespread use of cement in building [5–9]. The high percentage of CO_2 emissions in the OPC manufacture process is associated with the limestone calcination process that is considered as one of the major cement ingredients [10]. The consumption of heat energy resulting in temperatures greater than 1400°C during the manufacturing process of the raw materials in the kiln has led to a high release of CO_2 [11–15].

Geopolymer cement has been used over the past decade as an alternative solution to cement because it provides a suitable use for industrial wastes by converting them into cementitious products via the alkali-activation process [16]. The use of geopolymer technology in building has greatly reduced cement consumption, cutting carbon pollution by up to 80 percent and therefore decreasing the cement industry's environmental impact. Also, to resolve concerns arising from the disposal of industrial materials by processing and repurposing them in geopolymer production [17], geopolymer cements improve structural performance by enhancing durability and compressive strength, improving resistant against acid, and structural performance under elevated temp curing conditions. The kind and quantity of binder ingredients employed, the alkaline activator utilized, and the curing conditions utilized influence and govern these qualities [17]. Geopolymers seem to be inorganic alumina-silicate materials that have been formed into three-dimensional polymeric chains using alkaline activator solutions [18]. GGBFS, a granular by-product, nonmetallic, and glassy from the iron producing industry, is one of the most frequently utilized alumina-silicate components in the preparation of geopolymer cement. Alumina, silicates, and calcium, as well as other bases, make up the majority of it [19, 20].

Metakaolin (MK) is an amorphous alumina-silicate clay that is formed thermally by calcining kaolinite clay at 500–800 degrees centigrade in a dehydroxylation process [21]:

$$\mathrm{Al2Si2O4\,(OH4)} \quad \longrightarrow^{7} 00-800^{\circ}\mathrm{C}\ \mathrm{Al2O3.2SiO3} + \mathrm{2H2OKaolin}\ \ \mathrm{Metakaolin}. \tag{1}$$

Kaolin clay seems to be a fine, white clay mineral that is often used in porcelain production [22]. The type and chemical composition of these basic minerals greatly depend on their source. In addition to other elements such as alkaline activators and curing conditions, this variation has a significant influence on the pace of strength development and chemical processes of geopolymer cement [23]. As a result, in terms of generating a product with consistent precise desirable qualities, the manufacturing process of geopolymers necessitates a higher level of quality control than that of traditional Portland cement [24]. Once Portland cement is completely substituted by alkaline activated cements, Bernal and Provis [25] and Juenger et al. [26] found that GGBFS-based geopolymer concretes have strong mechanical performance and generate durable concrete with a low environmental impact. Despite this, the alkali-activated GGBFS-based geopolymer sets quickly and has poor workability significant microcracks, efflorescence drying shrinkage, and dry shrinkage [27, 28], and low carbonation resistant [29]. MK was employed in the early geopolymers improvement owing to its strong reactivity with alkaline activators and pure alumina-silicate amount that aids create a greater degree of geopolymerisation since its high amorphous phase amount and finer particle size [24]. Once heated, the geopolymer-based MK caused more matrix degradation than the fly ash geopolymer. The major source of the damage was discovered to be the prominent mesopores in the geopolymer-based MK matrix, which prevent moisture from escaping when heated. Although in the situation of fly ash, the geopolymer matrix has a significant number of micropores that allow moisture to escape once heated, causing little degradation to the geopolymer matrix [30, 31]. The fly ash-based geopolymer, on the contrary, revealed a problem with the curing conditions. To establish structural integrity and increase strength, a high-temperature curing process is required [32].

Owing to the facts presented throughout the introductory section, several researchers have investigated the formulations of novel blended binders made from two different materials in order to overcome the aforementioned shortcomings of such binders [33–35]. The new binders have been created by mixing aluminosilicate elements with the slag binder, including MK and fly ash (FA). In comparison to binders in which only the aluminosilicate precursors have been activated, the activation of these two materials leads to enhancements in several characteristics; additionally, such mixed binders advance an original microstructure with the coexistence of Ca-rich and Na-rich reaction products [25]. Once comparison with binders made from a raw material, including geopolymer-based-MK, laminar structures composition, and blending GGBFS with alumina-silicate substances under great alkalinity situations resulted in a greater dissolution rate of siliceous structures, thus enhancing the system's durability and stability [24].

A study conducted on the mechanical properties of GGBFS and MK geopolymer mortar found that the mixture of 20% GGBFS and 80% MK gave the highest compressive strength [36], while the difference in NaOH amount had affected the resultant compressive strength in relation to GGBFS amount; it has been detected that increasing the NaOH amount from 2.0 M to 1.2 M reduces compressive strength unless more GGBFS amount is added to the mixture. Whilst Bernal [25] discovered that the addition of MK caused a substantial increase in the compressive strength. Burciaga-Díaz et al. [37] detected that the compressive strength for the GGBFS and MK geopolymer pastes increased with high GGBFS amounts up to 100%, and Rao and Raja [38] found the same for GGBFS and MK geopolymer concrete. The maximum compressive strength was also obtained at 0% MK + 100% GGBFS of 52.0 $\mathrm{N/mm^2}$. Nevertheless, studies looked only at the impact of a low molar proportion of NaOH, but they did not investigate the strength of the results under a high molar proportion such as 12 M.

Thus, this investigation aimed to determine the molarity impact of sodium hydroxide on strength under low and high alkalinity. It also focused on the significant role that water plays in the dissolution stage of the geopolymerisation

Table 1: Chemical analysis of undisturbed materials used using EDXRF.

Ingredients	CaO	Al_2O3	SiO_2	Na_2O	MgO	K_2O	TiO_2	Fe_2O_3	BaO	SO_3
OPC	65.829	1.704	24.476	1.414	1.342	0.688	0.405	2.524	0.177	—
GGBFS	38.744	4.673	36.467	3.124	4.056	0.528	0.808	0.064	0.150	—
MK	0.166	41.720	41.193	—	—	0.088	1.402	0.331	0.121	0.067

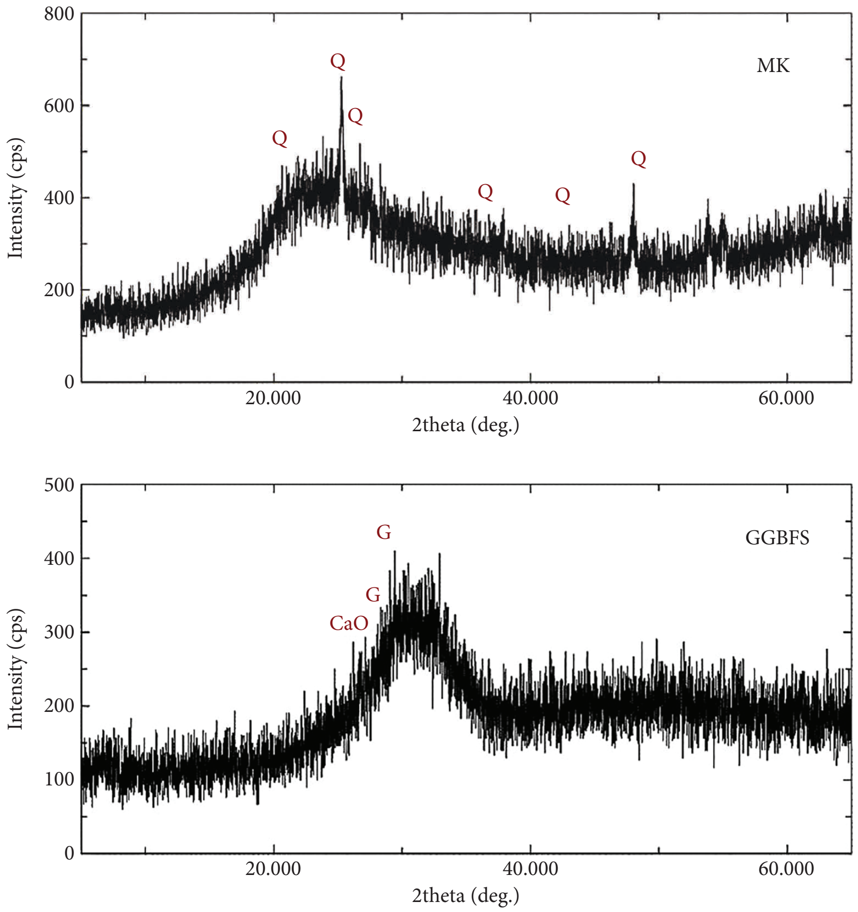

Figure 1: XRD diffractions forms for the utilized materials, GGBFS and MK. G = gypsum and Q = quartz.

process and, consequently, the compressive strength. The work sets out to investigate various water amounts that were added to various binder proportion mixes. The study also aimed to discover the influence of combined factors (molar proportion, water amount, and binder proportion) on the strength of the mix to optimize the mix design proportions. This research focuses on finding how far can geopolymer replace cement by studying the compressive strength, setting time, and microstructure of the produced samples.

2. Research Methodology

2.1. Materials Used and Mix Constituents. Commercially, GGBFS powder was obtained from Hanson Cement Ltd. in the UK on January 11, 2017, whilst MK powders were obtained from BASF Chemical Company, Canada. GGBFS and MK at chemical analysis demonstrated in Table 1 were utilized as the main raw materials. MK consists mainly of 41.193 percent silica and 41.720 percent alumina with just 0.166 percent CaO, though GGBFS consists mostly of calcium oxides with a ratio of 38.744 percent and silica amount of 36.467 percent with just 4.673 percent alumina. The powder XRD pattern of raw materials demonstrated that both MK and GGBFS are amorphous with only a noticeable semi-crystalline peak of quartz (Q) was detected at 25° (2 theta) in MK, whereas gypsum (G) and lime (CaO) at around 28° (2 theta) were detected in GGBFS, as shown in Figure 1. Alternatively, SEM analysis of the raw materials (Figure 2) illustrates that GGBFS consists primarily of angular particles, whereas MK seems to have a platy particle shape; additionally, the MK particle seems to have a large surface area with a small size, which increases its water requirements and reactivity when compared to GGBFS.

To make the geopolymer mortar-based slag/metakaolin, GGBFS was chosen as the primary binder (b) in this research, and it has been partially substituted by MK, as indicated in Table 2. The reference mixtures (C refers to the reference sample with cement only, while CS refers to the

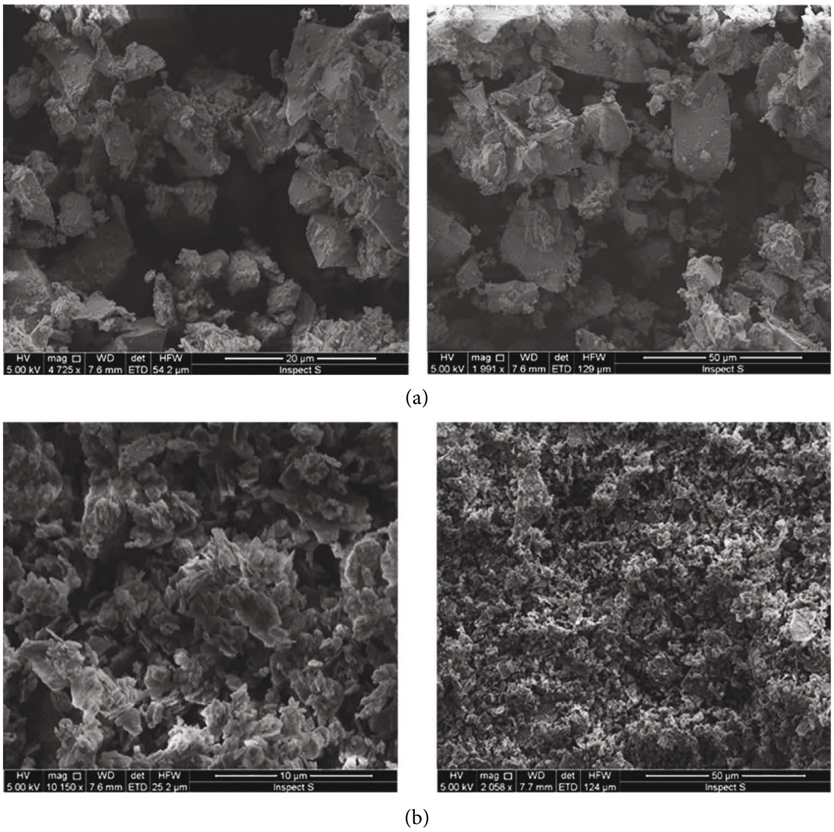

(a)

(b)

Figure 2: SEM observations for powders (a) GGBFS and (b) MK.

reference sample with cement and superplasticizer) for the comparison with geopolymer mortar were made with ordinary Portland CEM II (32 grade). In the preparation of the mortar mixes, natural dry sand with a specific gravity = 2.62 Mg/m^3 and a particle size = 0/2 FP washed plastering sand Gf85 [39] has been utilized as fine aggregate. As an alkaline solution (Al), a combination of sodium silicate (SS) and sodium hydroxide (SH) has been employed to prepare the geopolymer specimens. The sodium silicate solutions had a molar ratio of $SiO_2 : Na_2O$ of 2 : 1, a water content of 60%, and a specific gravity of 1.5. Sodium hydroxide has been created from pellets (98 percent pureness) dissolved in water (w) at two different molar amounts, 12 M and 0.3 M, which have been selected after conducting many trials to obtain the best molar amount (12 percent amount of solutions) to see the impact of concentrations in different molarities and percentages on the compressive strength. Distilled water was added to all mixtures, and to keep on workability, superplasticizer (S) has been utilized at 1% in select mixtures, as indicated in Table 2.

2.2. Specimen Synthesis and Experimental Procedures

2.2.1. Preparation of Alkaline Activator Solutions. Sodium silicate and sodium hydroxide were used to make the alkaline solutions. Sodium hydroxide has been initially made by dissolving NaOH granules in distilled water and letting it cool for 24 hrs at room temp. To test the effect of solution molar ratio on compressive strengths, the NaOH solution has been produced in two amounts: 12 molar solution and 12 percent (0.3 molar). To make the 12 molar solution, 480 gm of NaOH solid granules ($12 \times 40 = 480$) have been dissolved in one litre of pure water (in which 40 was the NaOH molecular weight). The 12 percent NaOH solution has been made by dissolving 12 gm of NaOH granules in a litre of water. Sodium silicate has been applied in two various proportions. First, it has been applied at mass proportion of 2.5 (sodium silicate mass to sodium hydroxide mass) and then added at 2.0 mass ratio. After that, water has been inserted into the alkaline activator solutions in two different quantities as given in Table 2, and the mixture has been allowed to sit for a few minutes before being used in the geopolymer mixture.

2.2.2. Mix Proportions of Specimens. The raw materials have been mixed at specific mass proportions of GGBFS/(GGBFS + MK) to make the cubic mortar samples as shown in Table 2, and all mixtures were made with a total binder amount of 775 kg/m^3. Dried sand was added at a mass proportion of 1.5 sand to the binder (GGBFS + MK), while activator was added at a mass proportion of 0.4 activator/binder, whiles water/binder ratio was first 0.4 and then decreased to 0.2 with the addition of 1% superplasticizer, as shown in Table 2.

Table 2: Combination composition of mortars OPC and slag/MK-based geopolymer utilized in the current investigation.

MixID	Ingredients' quantity (kg/m^3)										
	Binder	OPC	GGBFS	MK	Sand	SH (12%)	SH (12 M)	SS	w/b	S	Al/b
100 G	775	0	775	0	1162.5	88.57	0	221.43	0.4	0	0.4
90 G	775	0	697.5	77.5	1162.5	88.57	0	221.43	0.4	0	0.4
80 G	775	0	620	151	1162.5	88.57	0	221.43	0.4	0	0.4
70 G	775	0	542.5	232.5	1162.5	88.57	0	221.43	0.4	0	0.4
60 G	775	0	465	310	1162.5	88.57	0	221.43	0.4	0	0.4
50 G	775	0	387.5	387.5	1162.5	88.57	0	221.43	0.4	0	0.4
100 GM	775	0	775	0	1162.5	0	88.57	221.43	0.4	0	0.4
90 GM	775	0	697.5	77.5	1162.5	0	88.57	221.43	0.4	0	0.4
80 GM	775	0	620	151	1162.5	0	88.57	221.43	0.4	0	0.4
70 GM	775	0	542.5	232.5	1162.5	0	88.57	221.43	0.4	0	0.4
60 GM	775	0	465	310	1162.5	0	88.57	221.43	0.4	0	0.4
50 GM	775	0	387.5	387.5	1162.5	0	88.57	221.43	0.4	0	0.4
100 GS	775	0	775	0	1162.5	88.57	0	221.43	0.2	7.75	0.4
90 GS	775	0	697.5	77.5	1162.5	88.57	0	221.43	0.2	7.75	0.4
80 GS	775	0	620	151	1162.5	88.57	0	221.43	0.2	7.75	0.4
70 GS	775	0	542.5	232.5	1162.5	88.57	0	221.43	0.2	7.75	0.4
60 GS	775	0	465	310	1162.5	88.57	0	221.43	0.2	7.75	0.4
50 GS	775	0	387.5	387.5	1162.5	88.57	0	221.43	0.2	7.75	0.4
100 GMS[1]	775	0	775	0	1162.5	0	88.57	221.43	0.2	7.75	0.4
95 GMS	775	0	736.25	38.75	1162.5	0	88.57	221.43	0.2	7.75	0.4
90 GMS	775	0	697.5	77.5	1162.5	0	88.57	221.43	0.2	7.75	0.4
85 GMS	775	0	658.75	116.25	1162.5	0	88.57	221.43	0.2	7.75	0.4
80 GMS	775	0	620	151	1162.5	0	88.57	221.43	0.2	7.75	0.4
75 GMS	775	0	581.25	193.75	1162.5	0	88.57	221.43	0.2	7.75	0.4
100 C	775	775	0	0	1162.5	0	0	0	0.4	0	0
100 CS[2]	775	775	0	0	1162.5	0	0	0	0.2	7.75	0

100 refer to the GGBFS proportion used in relation to the total binder; G is GGBFS; M refers to the use of 12 molar NaOH solution, S refers to the use of superplasticiser. C is cement and S refers to the use of superplasticiser.

Table 3: The average compressive strengths in MPa after seven days.

Compressive strength (MPa)							
Mix ID GGBFS/(GGBFS + MK) (%)	G	GM	GS	Mix IDGGBFS/(GGBFS + MK) (%)	GMS	Mix ID	Control mixes
100	30.0	56.6	64.3	**100**	63.5	**C**	31.8
90	23.8	32.7	55.9	**95**	77.8	**CS**	8.4
80	4.0	8.6	49.6	**90**	60.4		
70	2.0	7.3	15.1	**85**	69.1		
60	1.8	7.5	9.2	**80**	61.8		
50	1.8	8.5	4.8	**75**	69.4		

Note: the mix designs given are found by the number in the first column with the letter in the first raw above to have the same mix design in Table 3.

2.2.3. Mixing and Casting Procedure. The alkali activators were first prepared a few minutes earlier and blended together. After that, the free water was inserted to blend well. GGBFS and MK were first weighted separately and then blended together for approximately 2 min. The alkali activator solution was then added to the blended mixture of GGBFS and MK and all mixed together for 2-3 minutes. Next, dried fine aggregates are applied to the previous combination and blended well for another 120 seconds. Eventually, the samples have been poured into PVC cubic moulds of 4 × 4 × 4 cm dimensions, left uncovered at a temp (27 ± 2°C with 0% RH) for 24 hours, and then demoulded and cured under different temperature conditions.

Table 4: Masses and compressive strengths for 95 percent GMS amount at 28 curing days.

Specimens	Compressive strengths (MPa)	Masses (g)
1	86.1	133.5
2	70.5	133.3
3	91.7	134.3

Hardened geopolymer mortar: the average strength of concrete of three 4 cm side cubes has been evaluated in the laboratory utilizing a universal testing machine (UTM) in line with BS EN 196-1 2005 [40] at a loading rate of 0.40 MPa/sec.

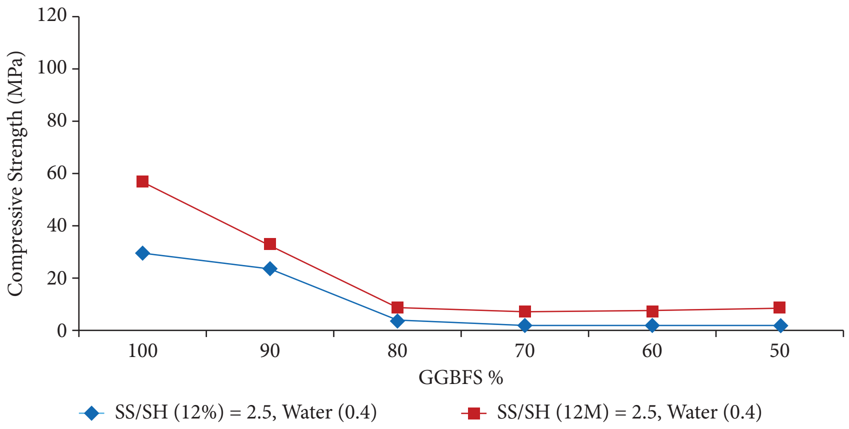

Figure 3: The impact of NaOH molar proportion on the compressive strengths at 7 curing days.

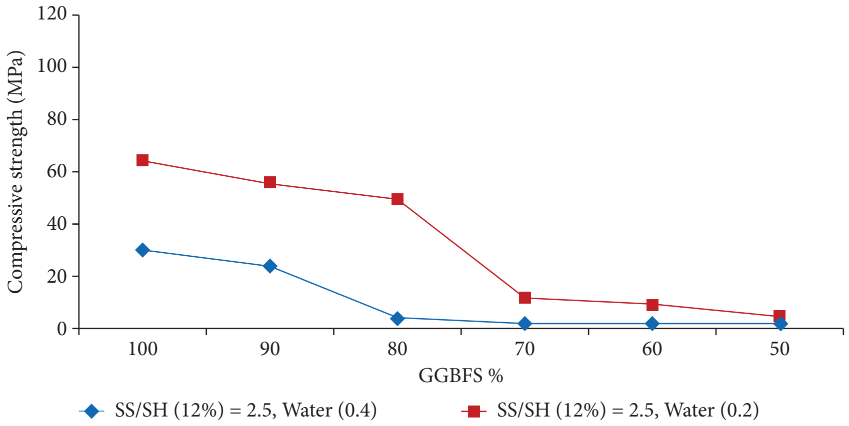

Figure 4: The impact of superplasticiser and low water amount on compressive strengths at 7 curing days.

Analytical analysis of geopolymer: the MK and GGBFS microstructure geopolymer combinations have been studied using a scanning electron microscope (SEM). To ensure that specimens seem to be fully free from water, small pieces have been hammered from the paste's core and dried at 40 degrees centigrade for four hours. The basic chemical analysis of OPC, MK, and GGBFS, and the XRD forms for both GGBFS and MK, have been determined using powder X-ray fluorescent and X-ray diffraction examinations.

3. Results and Discussion

In this section of the research, we present, through the tables, the compressive strength results for each of the previously pelleted samples in Table 3, in which we used GGBS and MK as alternative materials for cement, adding to them solutions of sodium hydroxide and sodium sulphate in order to activate the reaction between them. Also, tests were conducted on two samples of cement as a binder in order to compare with the previous samples. Therefore, the results showed the following.

Table 3 shows the compressive strength obtained after 7 days for different mix designs.

In Table4, the masses have been taken for the mix design of 95 GMS since it is the optimum mix design that gives the highest compressive strength among the other mixes. And, as shown in Table 4, the mass with a small amount can change the compressive strength of the geopolymer.

3.1. The NaOH Molar Proportion Influence. Increasing sodium hydroxide concentration from 12% to 12 M enhanced the compressive strengths of the geopolymer (Figure 3). The compressive strengths at seven curing days increased significantly from 30 MPa for the 100G mix to 56.6 MPa for the 100 GM mix and from 23.8 MPa for the 90G mix to 32.7 MPa for the 90 GM mix, which have all been greater than 31.8 MPa for that of mix C (Table 3).

The great amount of NaOH in alkaline solutions boosts silica and alumina particle dissolution and promotes the development of both CSH and geopolymer gels, which enhances compressive strengths. Once the calcium content is low, as in 80–50 percent GGBFS, the content of hydroxyl ions rises, preventing Ca^{2+} dissolution. As a result, the dissolved aluminum and silicate particles form geopolymer gel, inhibiting CSH production and resulting in poor compressive strength. However, once the calcium

Table 5: Various GGBFS amount with various water proportions.

Mix IDGGBFS/(GGBFS + MK) (%)	Masses (g)		
	G	GS	GMS
100	127.5	136.6	138.8
90	126.8	134.6	136.9

Note: the mix designs mentioned are found by the number in first column with the letter in the first raw above to have the same mix design in Table 3.

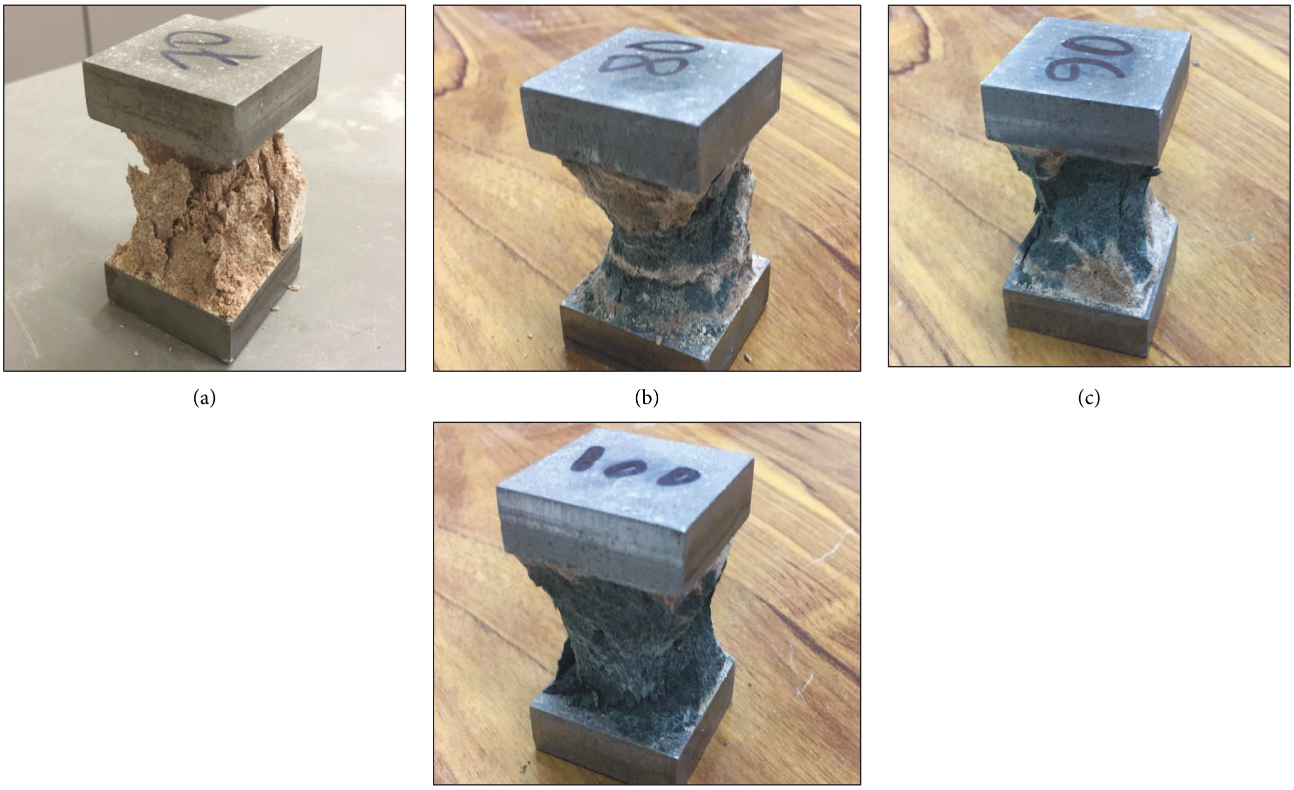

(a) (b) (c) (d)

Figure 5: The impact of water amount and super plasticisers on different GGBFS amount mixture's structure.

concentration is sufficient, as in 90 and 100 percent GGBFS, there might be enough dissolved Ca^{2+} to produce CSH and geopolymer gels, leading to increased strengths. Once the NaOH content is lower (12 percent), less hydroxyl ions have been generated, causing more dissolved Ca^{2+} and less dissolved aluminum and silicates particles owing to the low alkalinity environment, leading in more CSH gel and less geopolymer gel, which lead to poor compressive strength [36, 41]. Furthermore, as the amount of alumina-silicate rises, the potential for Si–O–Si and Si–O–Al bonding increases and, therefore, does the necessity for high alkali content solutions to enhance the dissolution of Si–O–Al and Si–O–Si bonds and thus the precipitation of cementitious reactions [42]. The requirement for activator is substantially lower at low MK concentrations (90–100 percent GGBFS).

Furthermore, a progressive rise in compressive strength was from 35.3 MPa at 50 percent GGBFS to the optimal magnitude of 44.0 MPa at 100 percent GGBFS, utilizing a 8 M sodium hydroxide solution at ambient curing temps [38]. Although there was no substantial increase in compressive strength between 50 and 80 percent GGBFS in Figure 3, there had been a considerable rise once GGBFS was increased to 90 and 100 percent.

3.2. The Impact of Low Water Amount. Figure 4 shows the impact of low water content with 1% superplasticizer on the compressive strength of geopolymer mortar cubes.

The compressive strength was enhanced by halving the quantity of water (0.2 water/binder proportion). It boosted the strength of specimens 100GS = 64.3 MPa and 90GS = 55.9 MPa, which is two times higher than the strength of specimens 100G and 90G (Table 3), while it increased the strength from 3.97 MPa at 80 G to 49.60 MPa at 80 Gs with enough workability for moulding, which is higher than the control mix C. Decreasing water amount

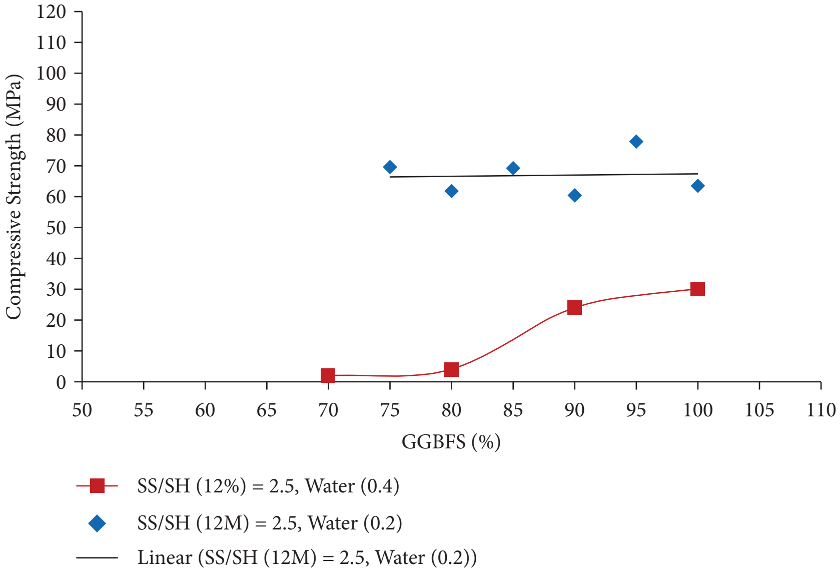

Figure 6: Boosting the mixture ratio after 7 curing days without RH.

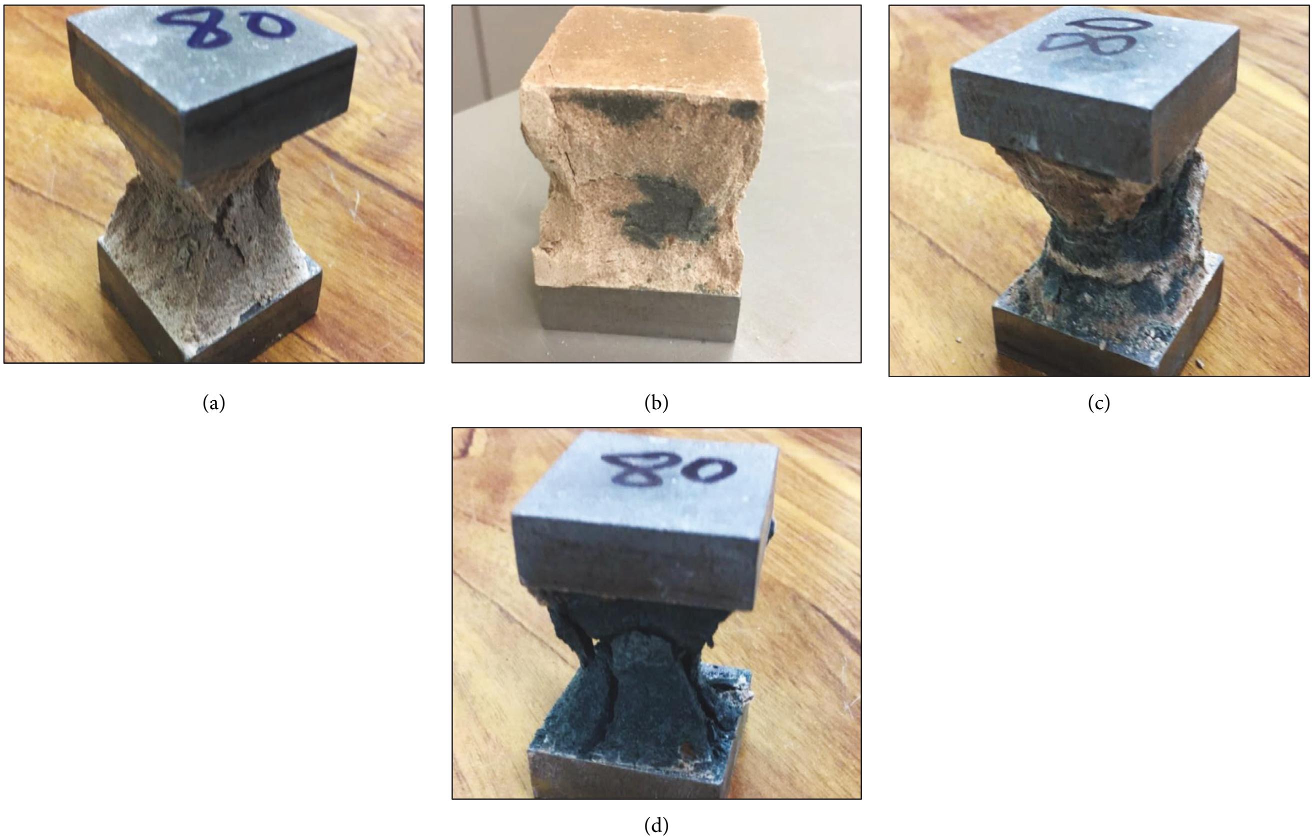
(a)

(b)

(c)

(d)

Figure 7: The impacts of various NaOH molar proportion and water amount on the geopolymerisation processes (specimens with 80 and 20 percent of GGBS and MK, respectively) the pictures have been lected after conducting compressive strengths test; (a). 40% water proportion, 12% NaOH; (b). 12 M NaOH, 40% water proportion (c). 1% SP, 20% water proportion, 12% NaOH; (d). 12 M NaOH, 20% water proportion, 1% SP.

aided reduce pores and voids in the systems leads to higher density structures (Table 5). The introduction of a superplasticizer helped give adequate workability for the reactions by dispersing the particles and releasing entrapped water by separating the agglomeration through the repulsion of similar charges [42]. However, raising the MK amount to

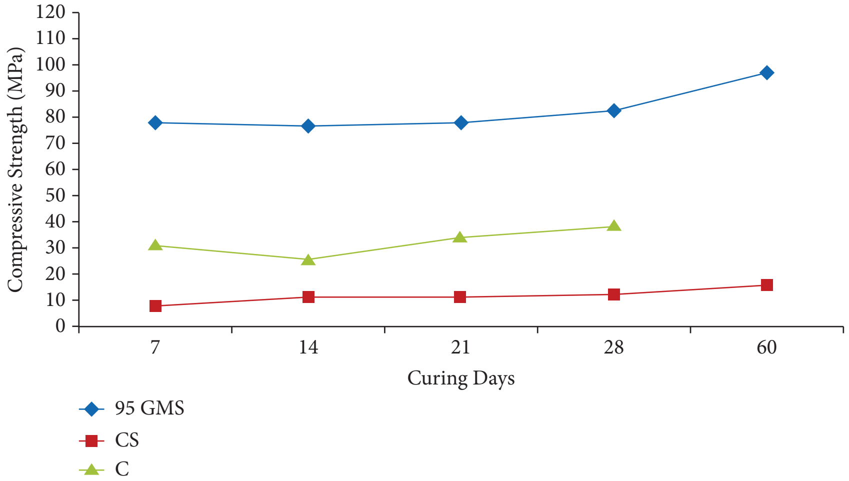

Figure 8: Compressive strength results for optimal mixture design and OPC reference mixtures during 7, 14, 21, 28 and 60 curing days.

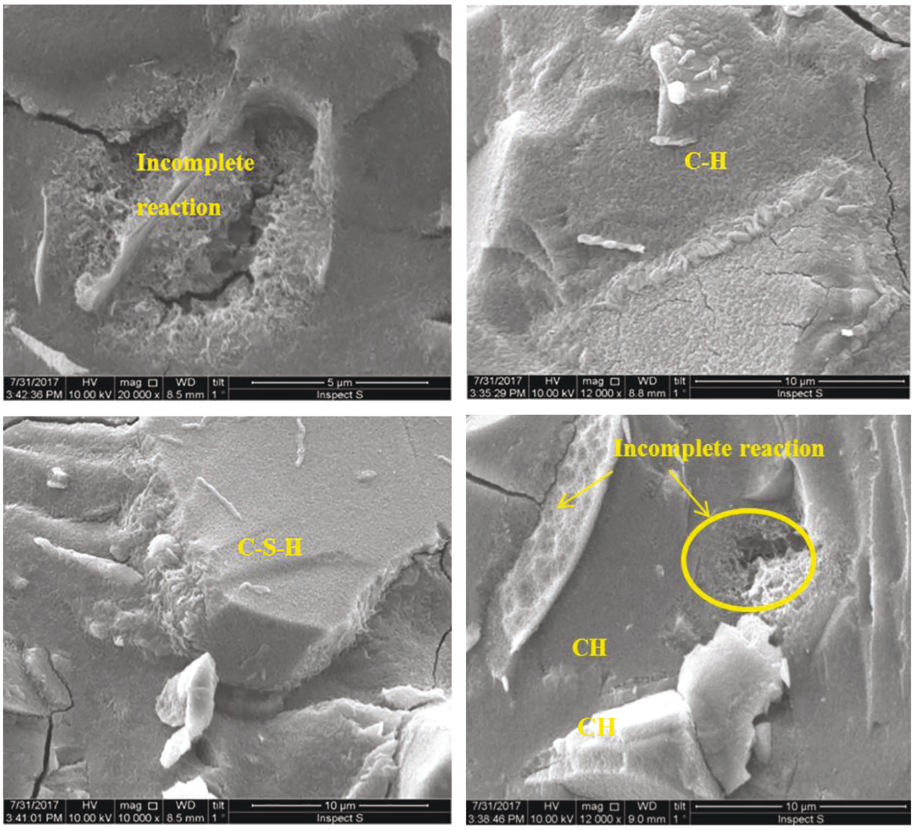

Figure 9: The SEM images for 95 GMS geopolymer paste at 7 curing days.

more than 30 percent (70 percent GGBFS or less) lowered strength magnitudes even after lowering the water quantity and applying 1% SP. It has been found that, at 30 percent MK, the mixture gets extremely dry despite the inclusion of superplasticizer. This is due to the increased surface area of MK, which necessitates a larger water amount so as to maintain sufficient water quantity and workability for the dissolving process.

Figure 5 demonstrates four specimens blended with various GGBFS amounts and constant water to binder proportions of 0.2. As samples gave various coloured areas, as shown in Figure 5, the darker sections relate to the reacted areas while the light-coloured sections relate to unreacted materials. Figure 5(a) demonstrates that the 70% GGBFS specimen had light-coloured sections that indicate unreacted areas. The sample failure seemed brittle in contrast to those with greater GGBFS levels, and this was attributable to a lack of water necessary to dissolve alumina-silicate owing to the higher MK content in the combination. As a result of the large number of open holes, it created a

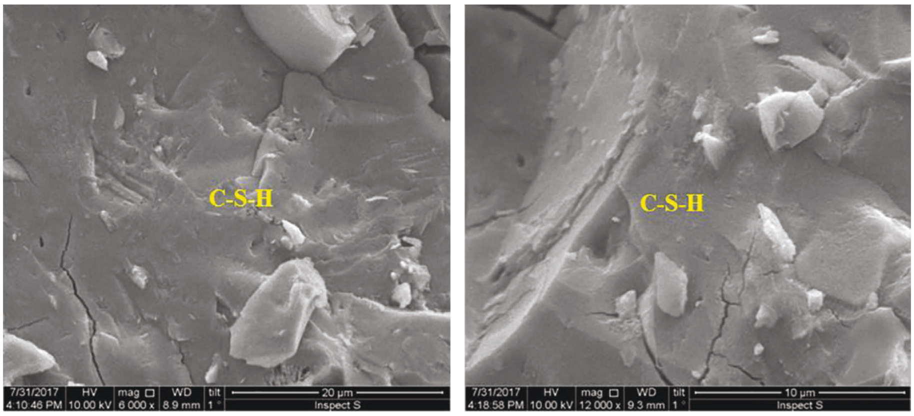

Figure 10: The SEM images for 90 GMS geopolymer paste at 7 curing days.

low-density geopolymer. Moreover, since MK possesses properties comparable to clay, it expands and contracts once exposed to water. As a consequence, specimens containing a high-level of MK had more open pores [43].

In contrast, the reaction process improved and formed more dark areas in samples with lower MK and higher GGBFS amounts, as shown clearly on the 80% GGBFS (Figure 5(b)), while it totally turned dark at 90 and 100% GGBFS amount (Figures 5(c) and 5(d)). Though several specimens lacked consistency in dark area distribution, it can be seen in the centre of the 80 percent specimen and around the margins of the 90 percent specimen. This indicates that the geopolymerisation process is nonuniform, as shown by the fact that the cubes' masses from the same mixture have been detected to be almost similar, despite the compressive strength of each cube being considerably different (Table 4).

3.3. *The Impact of Both Low Water Amount and High Molar Proportion.*

As illustrated in Figure 6, the combined impact of 12 M and 0.2 water amount with superplasticiser resulted in a considerable improvement in compressive strength. For the GGBFS amounts 100, 95, 90, 80, 85, and 75 percent, the compressive strength of cubes with low water amount and high molar proportion was spread around the magnitude 67 MPa. The overall impact of a 12 M sodium hydroxide solution and a little quantity of water increased the geopolymer's compressive strength and doubled it, notably for GGBFS and MK blended mixes, confirming MK's preferential dissolving in high alkaline solutions [25]. Due to the obvious high quantity of MK that has a large surface area and results in a dry mix owing to the high water requirements, the compressive strength cannot be evaluated at GGBFS levels lower than 75%. This resulted in inadequate workability to pour and compact the mixture in the mould.

The influence of both a large molar percentage of NaOH solutions and a small quantity of water on the geopolymerisation processing in terms of compressive strength and reaction products is shown in Figure 7. Increasing the molar proportions from 0.3 M to 12 M lead to production of dark grey colored patches in the cubic specimen (as shown in Figures 7(a) and 7(b)), which also caused a significant increase in compressive strength, especially at high GGBFS levels (Table 3). Decreasing the quantity of water to half the original value, on the contrary, resulted in substantially greater compressive strength, as seen by bigger dark regions in Figure 7(c). Despite this, the distribution of dark-colored patches was uneven across the specimen, indicating a nonuniform reaction process. Once the impacts of both low water quantity and high molar proportion were combined, the specimen fully changed color to a dark grey color (Figure 7(d)), and the compressive strength increased to greater levels (Table 3). As a consequence, the dark grey spots represent reaction products of the geopolymerisation process, which contribute to the high compressive strength.

3.4. *Comparison between Optimized and OPC Control Mix.*

In contrast to the two OPC reference mixtures, Figure 8 depicts the evolution of the optimal design proportions. The 95 GMS mix design produced much more strength in comparison with the two OPC mixtures. It possessed a compressive strength of 77.8 MPa at 7 curing days, which hovered around that amount till 21 days; then, the strength slightly improved to reach 82.7 MPa at 28 days, and it continued to increase till it reached 97.3 MPa at 60 curing days. The OPC mixture specimen of 0.2 (water/cement proportion) showed a little increase from 8.4 to 11.5 MPa between 7 and 14 days. After that, it held relatively stable strength at 12 MPa at 28 days and climbed to 15.9 MPa at 60 days. At the same time, the OPC mixes with 0.4 w/c proportion provide higher strength, reaching to 31.8 MPa at 7 days, while at 14 days the strength was 26 MPa since the cubes that were tested at 14 days were not from the same batch of the seven days' mix (same mix design with various cast dates); thus, the progress in the strength was not as expected. Subsequently, there was a gradual increase in strength to reach 38.4 MPa at 28 days.

3.5. *The SEM Analysis.*

Figures 9–11 illustrate the microstructure analysis of the three various blends at seven curing days, involving the optimal one (depending on compressive strength). The major reactions produced by GGBFS/MK binder with alkali activation lead to the creation of CH

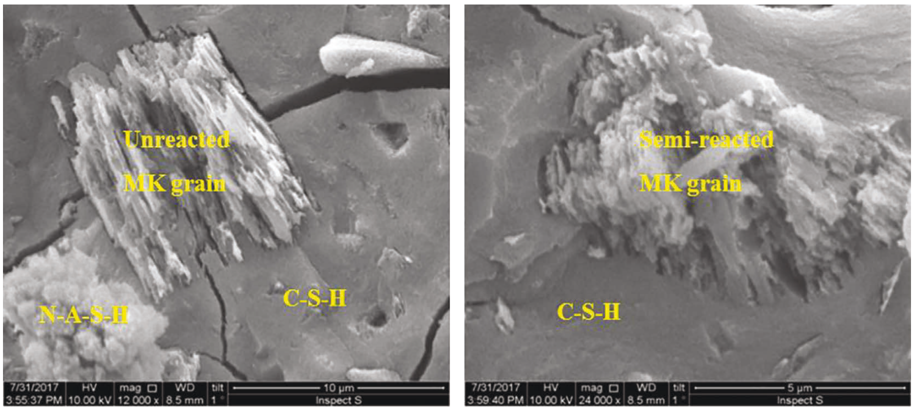

Figure 11: The SEM images for 85 GMS geopolymer paste at 7 curing days.

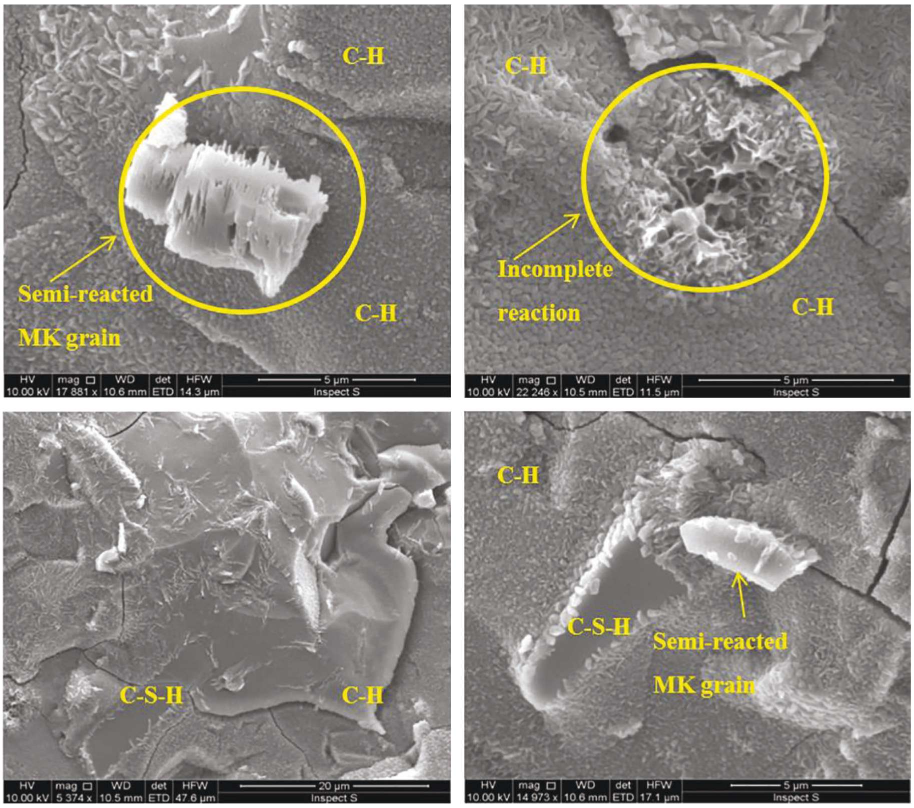

Figure 12: The SEM images for 95 GMS geopolymer paste at 35 curing days.

crystals and C–S–H gel, as shown in these images. The 85 GMS specimen microstructure is clearly illustrated in (Figure 11) the N–A–S–H gel as identified in [44]. Nonetheless, some unreacted MK particles and incomplete reaction regions have been found in the specimens with the produced gels, revealing the nonuniform reaction process distribution (Figure 11) that explains the large variance in the consequent compressive strength for the identical mixtures (as observed in Table 4).

Based on the lack of technicians available to do the test on that day, the SEM analysis for the next 28 days cannot be acquired; as a result, it was postponed until the next available day, that was 35 curing days after curing. Figure 12 shows that, after 35 curing days, more C–H crystals emerged inside the microstructure, whereas at high MK amounts, more C–S–H gel and sodium aluminosilicate hydrated gel (N–A–S–H) have been created (Figures 13 and 14). Because MK seems to be the main silicate and alumina source, increasing MK concentration increased the likelihood of more N–A–S–H gel formation rather than CH for the 90 GMS and 85 GMS specimens. C–H, as well as C–S–H, has been the primary products at lower MK levels (95 percent GGBFS). In the SEM pictures, microcracks were seen on the structural surface of all specimens. The external force applied by the hammer to create small parts appropriate for testing and the uncombined water

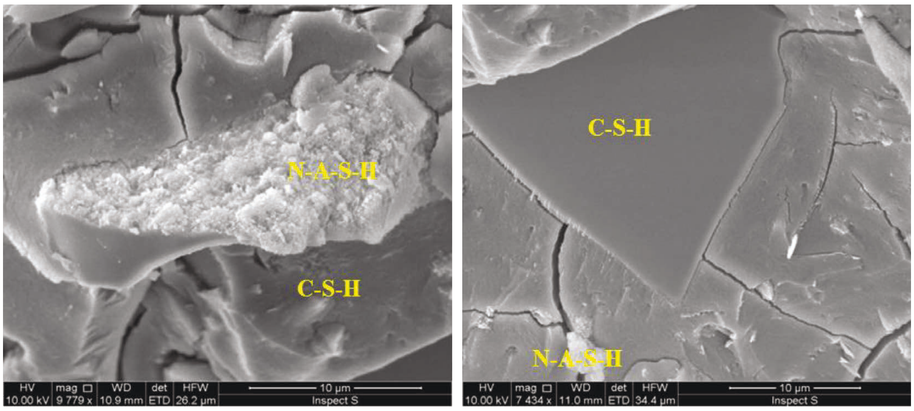

Figure 13: The SEM images for 90 GMS geopolymer paste at 35 curing days.

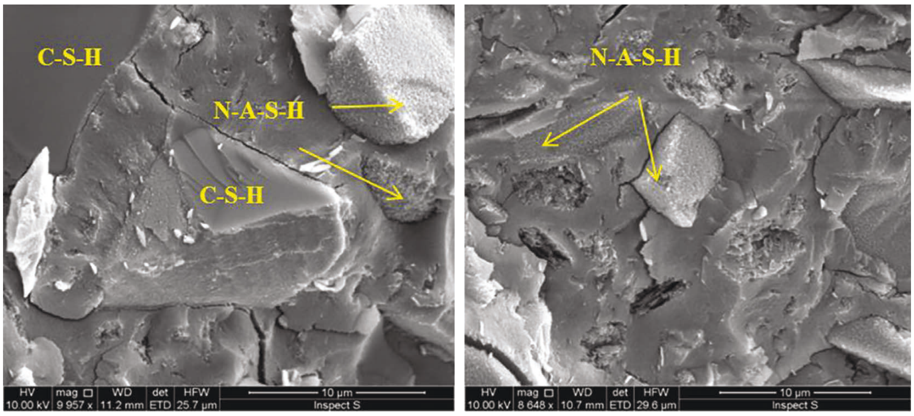

Figure 14: The SEM images for 85 GMS geopolymer paste at 35 curing days.

evaporated from the specimens when dried sample at 40 degrees centigrade in the furnace and then put in the microscope column vacuum, resulting in substantial shrinkage and thus microcracking, have all been reasons for their presence. Furthermore, the use of a low water/binder ratio in the mixture seems to be blamed.

4. Conclusion

In this research, different mix designs of GGBS and MK were prepared to seek the amount of compressive strength in comparison with OPC samples as well as the optimum mix design in terms of the compressive strength. The findings were as follows:

(i) In terms of optimized aluminosilicate dissolution species leading to the produced geopolymer, the high molar fraction of sodium hydroxide increased the cubes' compressive strength.

(ii) Alternatively, using a superplasticiser to reduce the quantity of water in the solution resulted in a denser structure by eliminating gaps and holes generated by leftover water and thereby increasing the mechanical qualities.

(iii) As a result of the combined influence of low water amount and high molar proportion with low curing temp, the optimal mixture (95 percent GGBFS + 5 percent MK) had been achieved.

(iv) The alkali-activated slag/MK geopolymer had a solid microstructure with no holes or cavities but some microcracks, according to SEM examination.

(v) C–S–H gel and CH crystals seemed to be prominent in the structure after 7 curing days, whereas (N–A–S–H) gel was found in the microstructure of greater MK amounts (85 GMS), along with some unreacted MK particles and incomplete reaction regions.

(vi) More C–H crystals grew inside the microstructure at 35 curing days, and more hydrated (N–A–S–H) gel and C–S–H gel have been created at great MK levels (90 GMS and 85 GMS).

(vii) Because MK was the primary silicate and alumina source, increasing MK concentration increased the likelihood of more N–A–S–H gel formation rather than C–H for the 90 GMS and 85 GMS specimens. C–H, as well as C–S–H, was the dominating product at lower MK amounts (95 GMS).

Data Availability

Most datasets generated and/or analysed in this study are included within the article. The other datasets can be obtained from from the corresponding author upon request.

Conflicts of Interest

The authors declare that they have no conflicts of interest.

Acknowledgments

This work was supported by Al-Mustaqbal University College (Grant number: MUC-E-0122). Mr Anmar Dulaimi and Mr Hassnen M Jafer are gratefully acknowledged for their help in providing the raw materials. This research was conducted in the labs of Liverpool John Moores University with the help of the technical staff.

References

[1] Y. Chen, F. Veer, and O. Copuroglu, "A critical review of 3D concrete printing as a low CO2 concrete approach," *Heron*, vol. 62, pp. 167–194, 2017.

[2] A. A. Adam, *Strength and Durability Properties of Alkali Activated Slag and Fly Ash-Based Geopolymer concrete*, RMIT Univ Melbourne, Melbourne Australian Forestry, 2009.

[3] K. Chen, D. Wu, L. Xia, Q. Cai, and Z. Zhang, "Geopolymer concrete durability subjected to aggressive environments–A review of influence factors and comparison with ordinary Portland cement," *Construction and Building Materials*, vol. 279, Article ID 122496, 2021.

[4] W. Li, E. D. Shumuye, T. Shiying, Z. Wang, and K. Zerfu, "Eco-friendly fibre reinforced geopolymer concrete: a critical review on the microstructure and long-term durability properties," *Case Studies in Construction Materials*, vol. 16, Article ID e00894, 2022.

[5] D. N. Huntzinger and T. D. Eatmon, "A life-cycle assessment of Portland cement manufacturing: comparing the traditional process with alternative technologies," *Journal of Cleaner Production*, vol. 17, no. 7, pp. 668–675, 2009.

[6] W. K. Tuama, M. M. Kadhum, N. A. Alwash, Z. S. Al-Khafaji, and M. S. Abdulraheem, "RPC effect of crude oil products on the mechanical characteristics of reactive-powder and normal-strength concrete," *Periodica Polytechnica: Civil Engineering*, 2020.

[7] X. S. Shi, F. G. Collins, X. L. Zhao, and Q. Y. Wang, "Mechanical properties and microstructure analysis of fly ash geopolymeric recycled concrete," *Journal of Hazardous Materials*, vol. 237, pp. 20–29, 2012.

[8] G. F. Huseien, J. Mirza, M. Ismail, S. K. Ghoshal, and M. A. M. Ariffin, "Effect of metakaolin replaced granulated blast furnace slag on fresh and early strength properties of geopolymer mortar," *Ain Shams Engineering Journal*, vol. 9, no. 4, pp. 1557–1566, 2018.

[9] M. Su, Q. Zhong, and H. Peng, "Regularized multivariate polynomial regression analysis of the compressive strength of slag-metakaolin geopolymer pastes based on experimental data," *Construction and Building Materials*, vol. 303, Article ID 124529, 2021.

[10] A. Naqi and J. G. Jang, "Recent progress in green cement technology utilizing low-carbon emission fuels and raw materials: a review," *Sustainability*, vol. 11, no. 2, p. 537, 2019.

[11] E. Gartner, "Industrially interesting approaches to "low-CO2" cements," *Cement and Concrete Research*, vol. 34, no. 9, pp. 1489–1498, 2004.

[12] H. S. Majdi, A. A. Shubbar, M. S. Nasr et al., "Experimental data on compressive strength and ultrasonic pulse velocity properties of sustainable mortar made with high content of GGBFS and CKD combinations," *Data in Brief*, vol. 31, Article ID 105961, 2020.

[13] A. A. Shubbar, M. Sadique, M. S. Nasr, Z. S. Al-Khafaji, and K. S. Hashim, "The impact of grinding time on properties of cement mortar incorporated high volume waste paper sludge ash," *Karbala International Journal of Modern Science*, vol. 6, no. 4, 2020.

[14] A. A. Shubbar, H. Jafer, M. Abdulredha et al., "Properties of cement mortar incorporated high volume fraction of GGBFS and CKD from 1 day to 550 days," *Journal of Building Engineering*, vol. 30, Article ID 101327, 2020.

[15] D. N. Jabbar, A. Al-Rifaie, A. M. Hussein, A. A. Shubbar, M. S. Nasr, and Z. S. Al-Khafaji, "Shear behaviour of reinforced concrete beams with small web openings," *Materials Today Proceedings*, vol. 42, 2021.

[16] S. A. Bernal, E. D. Rodríguez, A. P. Kirchheim, and J. L. Provis, "Management and valorisation of wastes through use in producing alkali-activated cement materials," *Journal of Chemical Technology and Biotechnology*, vol. 91, no. 9, pp. 2365–2388, 2016.

[17] S. Akçaözoğlu and C. D. Atiş, "Effect of granulated blast furnace slag and fly ash addition on the strength properties of lightweight mortars containing waste PET aggregates," *Construction and Building Materials*, vol. 25, no. 10, pp. 4052–4058, 2011.

[18] M. H. Al-Majidi, A. Lampropoulos, A. Cundy, and S. Meikle, "Development of geopolymer mortar under ambient temperature for in situ applications," *Construction and Building Materials*, vol. 120, pp. 198–211, 2016.

[19] M. Kaur and M. S. Naval, "Performance of ground granulated blast furnace slag concrete with partial replacement of sand by saw dust," *IOSR Journal of Mechanical and Civil Engineering*, vol. 2, no. 6, pp. 26–30, 2012.

[20] B. W. Tomkins, *Chemical Resistance of Geopolymer concrete against H2SO4 & NaOH,* University of Southern Queensland, Queensland, Australia, 2011.

[21] P. White, "Summary for policymakers," in *Intergovernmental Panel on Climate Change, editor. Clim Chang 2013 - Phys Sci Basis*, pp. 1–30, Cambridge University Press, Cambridge England, 2009.

[22] R. Siddique and M. I. Khan, *Supplementary Cementing Materials*Springer Science & Business Media, Heidelberg, Germany, 2011.

[23] S. M. A. Kabir, U. J. Alengaram, M. Z. Jumaat, A. Sharmin, and A. Islam, "Influence of molarity and chemical composition on the development of compressive strength in POFA based geopolymer mortar," *Advances in Materials Science and Engineering*, vol. 2015, pp. 1–15, 2015.

[24] S. A. Bernal, "Effect of the activator dose on the compressive strength and accelerated carbonation resistance of alkali silicate-activated slag/metakaolin blended materials," *Construction and Building Materials*, vol. 98, pp. 217–226, 2015.

[25] S. A. Bernal and J. L. Provis, "Durability of alkali activated materials: progress and perspectives," *Journal of the American Ceramic Society*, vol. 97, no. 4, pp. 997–1008, 2014.

[26] M. C. G. Juenger, F. Winnefeld, J. L. Provis, and J. H. Ideker, "Advances in alternative cementitious binders," *Cement and Concrete Research*, vol. 41, no. 12, pp. 1232–1243, 2011.

[27] Z. S. Al-Khafaji, Z. Al Masoodi, H. Jafer, A. Dulaimi, and W. Atherton, "The effect of using fluid catalytic cracking catalyst residue (FC3R) as A cement replacement in soft soil stabilisation," *International Journal of Civil Engineering & Technology*, vol. 9, pp. 522–533, 2018.

[28] T. Bakharev, J. G. Sanjayan, and Y.-B. Cheng, "Resistance of alkali-activated slag concrete to carbonation," *Cement and Concrete Research*, vol. 31, no. 9, pp. 1277–1283, 2001.

[29] D. L. Y. Kong, J. G. Sanjayan, and K. Sagoe-Crentsil, "Comparative performance of geopolymers made with metakaolin and fly ash after exposure to elevated temperatures," *Cement and Concrete Research*, vol. 37, no. 12, pp. 1583–1589, 2007.

[30] D. A. J. Hussain, "The fields of applying the recycled and used oils by the internal combustion engines for purposes of protecting the environment against pollution," *Journal of Advanced Research in Dynamical and Control Systems*, vol. 12, no. 01, pp. 698–706, 2020.

[31] A. Wardhono, D. W. Law, and A. Strano, "The strength of alkali-activated slag/fly ash mortar blends at ambient temperature," *Procedia Engineering*, vol. 125, pp. 650–656, 2015.

[32] F. Puertas and A. Fernández-Jiménez, "Mineralogical and microstructural characterisation of alkali-activated fly ash/slag pastes," *Cement and Concrete Composites*, vol. 25, no. 3, pp. 287–292, 2003.

[33] S. A. Bernal, J. L. Provis, B. Walkley et al., "Gel nanostructure in alkali-activated binders based on slag and fly ash, and effects of accelerated carbonation," *Cement and Concrete Research*, vol. 53, pp. 127–144, 2013.

[34] S. Kumar, R. Kumar, and S. P. Mehrotra, "Influence of granulated blast furnace slag on the reaction, structure and properties of fly ash based geopolymer," *Journal of Materials Science*, vol. 45, no. 3, pp. 607–615, 2010.

[35] R. Arellano Aguilar, O Burciaga Díaz, and J. Escalante García, "Lightweight concretes of activated metakaolin-fly ash binders, with blast furnace slag aggregates," *Construction and Building Materials*, vol. 24, no. 7, pp. 1166–1175, 2010.

[36] C. K. Yip, G. C. Lukey, and Van Deventer Jsj, "Effect of blast furnace slag addition on microstructure and properties of metakaolinite geopolymeric materials," *Ceramic Transactions*, vol. 153, pp. 187–209, 2004.

[37] O. Burciaga-Díaz, L. Y. Gómez-Zamorano, and J. I. Escalante-García, "Influence of the long term curing temperature on the hydration of alkaline binders of blast furnace slag-metakaolin," *Construction and Building Materials*, vol. 113, pp. 917–926, 2016.

[38] P. M. Rao and K. H. Raja, "Study of the properties of metakiolin and GGBS based geopolymer concrete," *International Journal of Civil Engineering & Technology*, vol. 8, 2017.

[39] S. Naganathan, S. Silvadanan, T. Y. Chung, M. F. Nicolasselvam, and S. Thiruchelvam, "Use of wastes in developing mortar–a review," *Advanced Materials Research*, vol. 935, pp. 146–150, 2014.

[40] B. Standard, *Methods of Testing Cement*, Determ Strength, 2005.

[41] E. Kim, *Understanding Effects of Silicon/aluminum Ratio and Calcium Hydroxide on Chemical Composition, Nanostructure and Compressive Strength for Metakaolin Geopolymers*, University of Illinois at Urbana-Champaign, Urbana, IL, 2012.

[42] M. Heikal, M. S. Morsy, and I. Aiad, "Effect of polycarboxylate superplasticizer on hydration characteristics of cement pastes containing silica fume," *Ceram Silikaty*, vol. 50, p. 5, 2006.

[43] P. Risdanareni, P. Puspitasari, E. Santoso, and E. P. Adi, "Mechanical and physical properties of metakaolin based geopolymer paste," *MATEC Web Conf*, vol. 101, p. 1021, 2017.

[44] Á Palomo, E. Kavalerova, A. Fernández-Jiménez, P. Krivenko, I. García-Lodeiro, and O. Maltseva, *A Review on Alkaline Activation: New Analytical Perspectives*, CSIC-Instituto de Ciencias de la Construcci{\'o}n Eduardo Torroja (IETCC), Madrid, Spain, 2015.